ROYAL SOCIETY OF CHEMISTRY

ChemComm

Bifunctional Electrocatalysis for CO2 Reduction via Surface Capping-Dependent Metal-Oxide Interactions

SCHOLARONE™
Manuscripts

COMMUNICATION

Bifunctional Electrocatalysis for CO$_2$ Reduction via Surface Capping-Dependent Metal-Oxide Interactions

Yueshen Wu[a,b], Xiaolei Yuan[a,b,c], Zixu Tao[a,b], Hailiang Wang*[a,b]

Multi-component materials are a new trend in catalyst development for electrochemical CO$_2$ reduction. Understanding and managing the chemical interactions within a complex catalyst structure may unlock new or improved reactivity but is scientifically challenging. We report the first example of capping ligand-dependent metal-oxide interactions in Au/SnO$_2$ structures for electrocatalytic CO$_2$ reduction. Cetyltrimethylammonium bromide capping on the Au nanoparticles enables bifunctional CO$_2$ reduction where CO is produced at more positive potentials and HCOO$^-$ at more negative potentials. With citrate capping or no capping, the Au-SnO$_2$ interactions steer the selectivity toward H$_2$ evolution at all potentials. Using electrochemical CO oxidation as a probe reaction, we further confirm that the metal-oxide interactions are strongly influenced by the capping ligand.

Electrochemical carbon dioxide (CO$_2$) reduction reactions are promising for valorizing CO$_2$ waste as an abundant and renewable carbon resource and for mitigating the adverse effects of increased CO$_2$ emissions on climate. Among all possible products of CO$_2$ electroreduction, carbon monoxide (CO) and formate (HCOO$^-$) are two valuable and easily accessible candidates.[1-3] Extensive research has been carried out to develop active and selective electrocatalysts for converting CO$_2$ to CO or HCOO$^-$.[2-5] Recent works have gone beyond single-component catalysts to more complex structures, such as bimetallic nanoparticles,[6-8] core-shell structures,[9, 10] molecule/nanocarbon hybrids[11, 12] and metal/oxide interfaces[13, 14] for higher activity and selectivity.

Metal-oxide interactions, a concept extensively studied for gas-phase catalysis,[15-17] has recently been investigated for enhancing electrocatalysis of CO$_2$ reduction.[10, 13, 14, 18-20] Both metals and metal oxides can be active catalysts for electrochemical CO$_2$ reduction reactions. Given the observation that CO can be produced by metal catalysts in the more positive potential region whereas HCOO$^-$ is formed on oxidized metal surfaces at more negative potentials,[21] it is possible to construct a CO/HCOO$^-$ bifunctional catalyst consisted of one metal and one metal oxide as active components, whose selectivity can be controlled by the applied potential. We have recently demonstrated such a catalyst utilizing win-win metal-oxide (Ag-SnO$_x$) cooperation that boosts both the CO$_2$-to-CO catalysis on the metal and the CO$_2$-to-HCOO$^-$ catalysis on the oxide.[13] Despite this progress, bifunctional CO$_2$ reduction electrocatalysts are still rare, possibly associated with the difficulty in managing multi-component interactions within a catalyst structure. A deeper understanding of metal-oxide interactions and their influences on catalytic properties therefore entails further investigation.

In this work, we studied different composites of Au and SnO$_2$ nanoparticles for CO$_2$ electroreduction. The Au-SnO$_2$ interactions were found to be strongly dependent on the capping ligand of the Au nanoparticles. In contact with SnO$_2$ nanoparticles supported on carbon nanotubes (SnO$_2$/CNT), both the capping-free Au (CF-Au) and citrate-capped Au (Cit-Au) nanoparticles give rise to adverse interactions that favor the competing hydrogen evolution reaction (HER). A substantial amount of H$_2$ is produced in the potential range of -0.50 to -1.00 V vs RHE. When the cetyltrimethylammonium bromide-capped Au (CTAB-Au) nanoparticles are used instead, HER is suppressed. The catalyst manifests a high selectivity for CO at -0.50 V and for HCOO$^-$ at -0.90 V, enabling bifunctional CO$_2$ reduction behavior. Using electrooxidation of CO as a probe reaction, we further show that the Au sites on the surface of CTAB-Au/SnO$_2$ are different from those of CF-Au/SnO$_2$ or Cit-Au/SnO$_2$. To the best of our knowledge, this is the first report on tailoring metal-oxide interactions and electrocatalytic properties via changing the capping ligand at the metal/oxide interface.
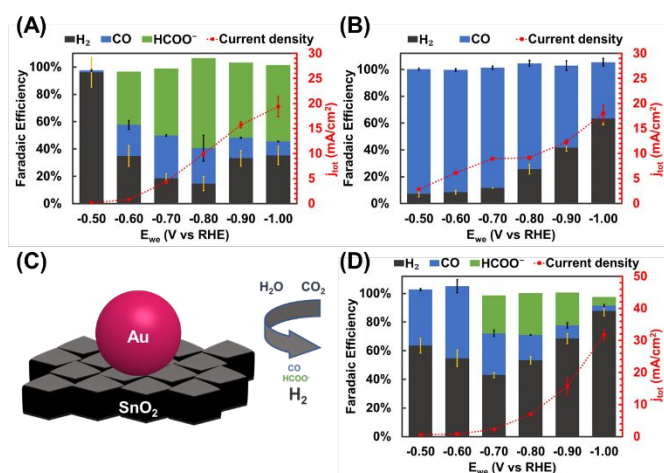
Figure 2. Potential-dependent catalytic performance of (A) SnO_2 and (B) CF-Au for electroreduction of CO_2. (C) Schematic illustration and (D) potential-dependent catalytic performance of CF-Au/SnO_2 for electroreduction of CO_2. Error bars represent standard deviations from multiple measurements.

Figure 1. (A, C) Schematic illustration and (B, D) potential-dependent catalytic performance of (A, B) CTAB-Au/SnO_2 and (C, D) Cit-Au/SnO_2 for electroreduction of CO_2. Error bars represent standard deviations from multiple measurements.

The Au/SnO_2 system without capping ligand was first investigated. Prior to the construction and measurement of this binary system, CF-Au and SnO_2 nanoparticles were respectively grown on CNTs (Figure S1, S2) for their intrinsic catalytic properties for CO_2 electroreduction to be assessed. CNTs are a widely-used support in electrocatalysis due to their high electrical conductivity and large surface area. [18, 22] In 0.5 M aqueous $KHCO_3$, SnO_2 catalyzes CO_2 reduction to $HCOO^-$ with an onset potential of -0.60 V vs RHE. The highest Faradaic efficiency (FE) for $HCOO^-$ is 66% achieved at -0.80 V with a total current density (j_{total}) of 9.91 mA/cm^2 (Figure 1A). CF-Au catalyzes CO_2 reduction to CO with the highest FE_{CO} of 93% and a j_{total} of 2.80 mA/cm^2 at -0.50 V (Figure 1B). These activity and selectivity results agree well with reports on Au and SnO_2 in the literature.[23, 24] The CF-Au/SnO_2 catalyst was constructed by growing CF-Au nanoparticles onto SnO_2/CNT (Figure 1C, S3). To our surprise, the catalytic performance of CF-Au/SnO_2 toward CO_2 reduction is far worse than a simple combination of CF-Au and SnO_2. H_2 is the major product throughout the potential range examined (Figure 1D). The highest FE_{HCOO^-} and FE_{CO} are only 29% and 50%, respectively.

We then explored the possibility of utilizing surface capping to modify metal-oxide interactions and to influence electrocatalytic CO_2 reduction. CTAB-Au nanoparticles were synthesized (Figure S2, S4A). They exhibit similar catalytic activity and selectivity toward CO_2-to-CO conversion as the CF-Au nanoparticles (Figure S5A). Remarkably, the CTAB-Au/SnO_2 mixture (Figure 2A, S6A, S6B) exhibits a potential-dependent bifunctional behavior for CO_2 electroreduction (Figure 2B). In the lower overpotential range, CO is the dominant product. At -0.50 V vs RHE, CO is produced with FE_{CO} = 96% and a j_{CO} of 0.26 mA/cm^2. In the more negative potential range, $HCOO^-$ is the major product, with the highest FE_{HCOO^-} = 65% achieved at -0.90 V together with a j_{HCOO^-} of 6.66 mA/cm^2. HER is suppressed to < 15% in FE in the potential range between -0.50 V and -0.90 V. As a comparison, we prepared Cit-Au nanoparticles from CTAB-Au nanoparticles via a reported ligand exchange method.[25] The absence of N element on the surface of the obtained Cit-Au
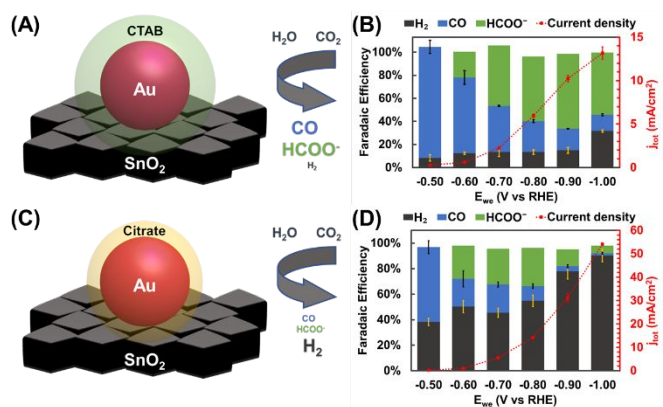
nanoparticles, as revealed by X-ray photoelectron spectroscopy (XPS), verifies successful substitution of CTAB with citrate ions (Figure S7). While Cit-Au shows similar electrocatalytic properties as CTAB-Au (Figure S5B), the Cit-Au/SnO_2 mixture (Figure 2C, S6C, S6D) exhibits a poor selectivity for both CO and $HCOO^-$ (Figure 2D). At -0.50 V, FE_{CO} is only 58%. At -0.90 V, FE_{H_2} reaches 78% and FE_{HCOO^-} is below 15%. This behavior is very similar to the case of the CF-Au/SnO_2 catalyst (Figure 1D), where HER dominates the reduction current in the entire potential range examined.

To understand the different catalytic properties of the three Au/SnO_2 systems, we performed a linear combination analysis to quantitatively capture the change of HER activity caused by the metal-oxide interactions as a function of the capping ligand on Au. We assume that in each Au/SnO_2 system the Au and SnO_2 components work independently and that the catalytic performance of the mixture is a simple addition of the two. Based on the fact that Au is predominant for CO production in the lower overpotential range and that SnO_2 provides the sole active sites for $HCOO^-$ production, the active contents of Au and SnO_2 in each Au/SnO_2 system are determined from the experimentally measured CO and $HCOO^-$ production rates at -0.50 V and -0.80 V, respectively (Table S1). Then the linear combination HER rate is calculated. Figure 3 compares FE_{H_2} and j_{H_2} calculated from the linear combination analysis with the experimentally-measured values for CF-Au/SnO_2, CTAB-Au/SnO_2 and Cit-Au/SnO_2. For all the three catalysts, the actual values deviate significantly from the linear combination values, suggesting that the Au-SnO_2 interactions strongly affect the catalysis. Notably, the three fall into two categories. For CTAB-Au/SnO_2, not only is the selectivity toward H_2 suppressed, the reaction rate is also notably lower than the simple addition of CTAB-Au and SnO_2 (Figure 3C and 3D). In contrast, CF-Au/SnO_2 and Cit-Au/SnO_2 both exhibit significantly higher activity and selectivity for HER (Figure 3A, 3B, 3E and 3F). These results support our conclusion that the surface capping ligands of Au nanoparticles strongly influence the interactions with SnO_2 and consequently alter the electrocatalytic properties for CO_2 reduction. In particular, CTAB mediates desirable Au-SnO_2

COMMUNICATION

interactions and enables product-selectable dual-mode CO_2 electroreduction to CO and $HCOO^-$ over a single catalyst.
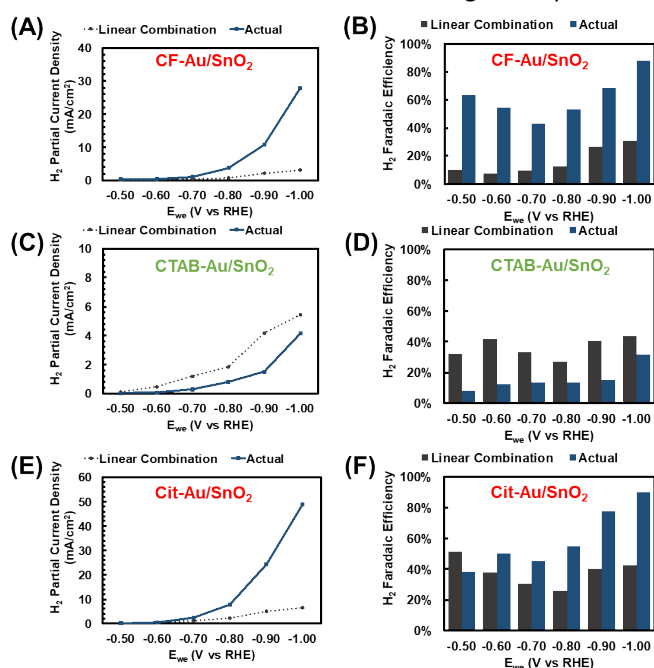
Figure 4. Comparison of (A, C, E) j_{H2} and (B, D, F) FE_{H2} between actual values and values calculated from linear combination analysis for (A, B) CF-Au/SnO₂; (C, D) CTAB-Au/SnO₂; (E, F) Cit-Au/SnO₂.

It is interesting to note that CF-Au, CTAB-Au and Cit-Au possess very similar catalytic properties for CO_2 electroreduction (Figure 1B, S5), yet their interactions with SnO_2 are quite different. While surface capping-dependent electrocatalytic activity and selectivity has been reported for Pt nanoparticles toward the oxygen reduction reaction,[26] this is the first time that capping ligand-mediated metal-oxide interactions in electrocatalysis are discovered. To further study how the metal-oxide interactions alter the properties of the catalytic sites, we chose electrooxidation of CO as a probe reaction to characterize the surface Au sites of the three Au/SnO₂ catalysts.[27-29] Au nanoparticles are known to catalyze CO electrooxidation in neutral aqueous solutions. Cyclic voltammograms were first recorded in CO-saturated 0.5 M aqueous KHCO₃ for the three kinds of Au nanoparticles with different capping states and the SnO₂ nanoparticles. SnO₂ itself is inactive toward CO electrooxidation of CO (Figure S8). The three kinds of Au nanoparticles exhibit almost identical onsets of CO oxidation at ~0.40 V vs RHE (Figure 4A), in line with earlier reports on CO electrooxidation on Au surface.[29, 30] This indicates that these Au nanoparticles with different capping states possess surface sites with similar chemical properties, which agrees with the observation that they show almost identical catalytic properties for CO_2 reduction. Coupled with SnO₂, the electrocatalytic activity of both CF-Au and Cit-Au for CO oxidation remains largely unaffected. The CTAB-Au/SnO₂, however, shows a much more positive onset potential at ~1.10 V. The drastically different activity of CTAB-Au/SnO₂ for CO electrooxidation confirms that the metal-oxide interactions in this catalyst is indeed different from those in the other two

Au/SnO₂ systems, which is consistent with the CO_2 electroreduction results. Given that the proposed rate-
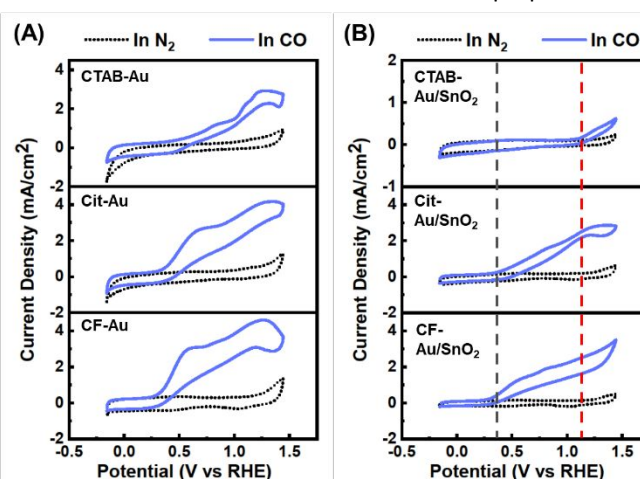
Figure 3. Cyclic voltammograms of (A) the three types of Au nanoparticles with different surface capping states and (B) the three Au/SnO₂ catalysts in N₂ and in CO in 0.5 M aqueous KHCO₃. Scan rate: 50 mV/s.

determining step for CO oxidation on Au involves the process of one-electron oxidation of surface-adsorbed CO,[31, 32] a more positive onset of this reaction implies increased CO binding affinity, which could be responsible for the observed HER suppression.

In summary, we for the first time demonstrated capping ligand-dependent metal-oxide interactions in electrocatalysis. The catalytic properties of our Au/SnO₂ model systems toward electrochemical CO_2 reduction reactions are strongly influenced by the presence and identity of capping ligands on the Au nanoparticles. Without capping ligands or with citrate as the capping ligand, HER is favored. With CTAB as the capping ligand, HER is suppressed and potential-dependent bifunctional catalysis toward CO and $HCOO^-$ is realized.

Conflicts of interest

There are no conflicts to declare.

Notes and references

1. J. M. Spurgeon and B. Kumar, *Energy & Environmental Science*, 2018, **11**, 1536-1551.
2. J. Qiao, Y. Liu, F. Hong and J. Zhang, *Chemical Society Reviews*, 2014, **43**, 631-675.
3. J. Artz, T. E. Müller, K. Thenert, J. Kleinekorte, R. Meys, A. Sternberg, A. Bardow and W. Leitner, *Chemical Reviews*, 2018, **118**, 434-504.
4. R. Francke, B. Schille and M. Roemelt, *Chemical reviews*, 2018, **118**, 4631-4701.
5. W. Zhang, Y. Hu, L. Ma, G. Zhu, Y. Wang, X. Xue, R. Chen, S. Yang and Z. Jin, *Advanced Science*, 2018, **5**, 1700275.
6. D. Kim, J. Resasco, Y. Yu, A. M. Asiri and P. Yang, *Nature Communications*, 2014, **5**, 4948.

7.   R. Kortlever, I. Peters, S. Koper and M. T. M. Koper, *ACS Catalysis*, 2015, **5**, 3916-3923.

8.   Z. Chang, S. Huo, W. Zhang, J. Fang and H. Wang, *The Journal of Physical Chemistry C*, 2017, **121**, 11368-11379.

9.   K. Sun, T. Cheng, L. Wu, Y. Hu, J. Zhou, A. Maclennan, Z. Jiang, Y. Gao, W. A. Goddard and Z. Wang, *Journal of the American Chemical Society*, 2017, **139**, 15608-15611.

10. W. Luc, C. Collins, S. Wang, H. Xin, K. He, Y. Kang and F. Jiao, *Journal of the American Chemical Society*, 2017, **139**, 1885-1893.

11. X. Zhang, Z. Wu, X. Zhang, L. Li, Y. Li, H. Xu, X. Li, X. Yu, Z. Zhang and Y. Liang, *Nature communications*, 2017, **8**, 14675.

12. M. Wang, L. Chen, T.-C. Lau and M. Robert, *Angewandte Chemie International Edition*, 2018, **57**, 7769-7773.

13. Z. Cai, Y. Wu, Z. Wu, L. Yin, Z. Weng, Y. Zhong, W. Xu, X. Sun and H. Wang, *ACS Energy Letters*, 2018, **3**, 2816-2822.

14. Q. Li, J. Fu, W. Zhu, Z. Chen, B. Shen, L. Wu, Z. Xi, T. Wang, G. Lu, J.-j. Zhu and S. Sun, *Journal of the American Chemical Society*, 2017, **139**, 4290-4293.

15. M. Behrens, F. Studt, I. Kasatkin, S. Kühl, M. Hävecker, F. Abild-Pedersen, S. Zander, F. Girgsdies, P. Kurr, B.-L. Kniep, M. Tovar, R. W. Fischer, J. K. Nørskov and R. Schlögl, *Science*, 2012, **336**, 893-897.

16. J. A. Rodriguez, S. Ma, P. Liu, J. Hrbek, J. Evans and M. Pérez, *Science*, 2007, **318**, 1757-1760.

17. K. An, S. Alayoglu, N. Musselwhite, S. Plamthottam, G. Melaet, A. E. Lindeman and G. A. Somorjai, *Journal of the American Chemical Society*, 2013, **135**, 16689-16696.

18. S. Huo, Z. Weng, Z. Wu, Y. Zhong, Y. Wu, J. Fang and H. Wang, *ACS Applied Materials & Interfaces*, 2017, **9**, 28519-28526.

19. G. O. Larrazábal, A. J. Martín, S. Mitchell, R. Hauert and J. Pérez-Ramírez, *ACS Catalysis*, 2016, **6**, 6265-6274.

20. S. Chu, P. Ou, P. Ghamari, S. Vanka, B. Zhou, I. Shih, J. Song and Z. Mi, *Journal of the American Chemical Society*, 2018, **140**, 7869-7877.

21. G. O. Larrazábal, A. J. Martín and J. Pérez-Ramírez, *The Journal of Physical Chemistry Letters*, 2017, **8**, 3933-3944.

22. Z. Weng, W. Liu, L.-C. Yin, R. Fang, M. Li, E. I. Altman, Q. Fan, F. Li, H.-M. Cheng and H. Wang, *Nano Letters*, 2015, **15**, 7704-7710.

23. S. Zhang, P. Kang and T. J. Meyer, *Journal of the American Chemical Society*, 2014, **136**, 1734-1737.

24. H. Mistry, R. Reske, Z. Zeng, Z.-J. Zhao, J. Greeley, P. Strasser and B. R. Cuenya, *Journal of the American Chemical Society*, 2014, **136**, 16473-16476.

25. J. G. Mehtala, D. Y. Zemlyanov, J. P. Max, N. Kadasala, S. Zhao and A. Wei, *Langmuir*, 2014, **30**, 13727-13730.

26. W. Liu and H. Wang, *Surface Science*, 2016, **648**, 120-125.

27. B. E. Hayden, D. Pletcher, M. E. Rendall and J.-P. Suchsland, *The Journal of Physical Chemistry C*, 2007, **111**, 17044-17051.

28. P. Rodriguez, D. Plana, D. J. Fermin and M. T. M. Koper, *Journal of Catalysis*, 2014, **311**, 182-189.

29. B. B. Blizanac, M. Arenz, P. N. Ross and N. M. Marković, *Journal of the American Chemical Society*, 2004, **126**, 10130-10141.

30. H. Kita, H. Nakajima and K. Hayashi, *Journal of Electroanalytical Chemistry and Interfacial Electrochemistry*, 1985, **190**, 141-156.

31. S. C. Chang, A. Hamelin and M. J. Weaver, *The Journal of Physical Chemistry*, 1991, **95**, 5560-5567.

32. G. J. Edens, A. Hamelin and M. J. Weaver, *The Journal of Physical Chemistry*, 1996, **100**, 2322-2329.